Catalysis Today 212 (2013) 75–80

Contents lists available at SciVerse ScienceDirect

Catalysis Today

journal homepage: www.elsevier.com/locate/cattod

Synthesis of solar light responsive Fe, N co-doped TiO_2 photocatalyst by sonochemical method

Tae-Ho Kim[a], Vicent Rodríguez-González[b], Gobinda Gyawali[a], Sung-Hun Cho[a], Tohru Sekino[c], Soo-Wohn Lee[a,*]

[a] Research Center for Eco Multi-Functional Nano Materials, Sun Moon University, Galsan-ri, Tangjung-Myon, Asan Chungnam, Republic of Korea
[b] Instituto Potosino de Investigación Cientifica y Tecnológica (IPICYT), División de Materiales Avanzados, Camino a la Presa San José 2055, Col. Lomas 4a. sección, C.P. 78216, SanLuis Potosí, S.L.P., Mexico
[c] Institute of Multidisciplinary Research for Advanced Materials (IMRAM), Tohoku University, Aoba-ku, Sendai, Japan

ARTICLE INFO

Article history:
Received 7 March 2012
Received in revised form 6 August 2012
Accepted 2 September 2012
Available online 23 October 2012

Keywords:
Photocatalyst
Sonochemical method
TiO_2
Co-doping
Solar light

ABSTRACT

Fe, N co-doped TiO_2 photocatalyst has been synthesized by sonochemical method. The as-prepared samples were characterized by XRD, TEM, UV–vis-DRS, XPS, FT-IR and physisorption of N_2. Experimental results show that the as-prepared TiO_2 photocatalyst has the anatase TiO_2 crystalline phase. The band-gap energy absorption edge of Fe, N co-doped TiO_2 shifted to longer wavelength as compared to commercial TiO_2–P25 and N–TiO_2. The specific surface area of the TiO_2 was increased to 75 $m^2\ g^{-1}$ with the doping of Fe and N ions into the TiO_2 framework. The photocatalytic activity of Fe, N co-doped TiO_2 for degradation of indigo carmine dye (ICD) under solar simulator was enhanced as compared to TiO_2–P25 and N–TiO_2.

1. Introduction

Since the discovery of the photosplitting of water on TiO_2 electrode by Honda and Fujishima in 1972 [1], TiO_2 photocatalyst has been widely applied for the removal of toxic agents in air and water [2–4]. However, TiO_2 photocatalysts operate fundamentally under UV light of wavelengths shorter than 400 nm, which means only 3–5% of solar light can activate these wide band-gap materials [5]. It is, therefore, required to develop a photocatalytic system, which can work even under visible light irradiation. Recently, many studies have been devoted to the modification of TiO_2 photocatalysts by the substitutional doping of metals or nonmetals in order to extend their absorption edge into the visible light region and to improve their photocatalytic activity [6–11]. Among them, metals or nonmetals doping is a practical approach because the properties of the material are largely determined by chemical nature of the atoms or ions and of the bonds between them. The most popular dopants for modification of the optical and photoelectrochemical properties of TiO_2 are nonmetal such as N [8,12], F [13], C [14], S [9,15] and Cl [16]. On the other hand, doping with metal ions is also a typical approach to extend the spectral response of TiO_2 to the visible light region by providing defect states in the band gap [17–19]. Transition metal ions such as Fe, Cr, Mo, La, V and W have been reported as effective in enhancing visible light photocatalytic activity [20–23]. Asahi et al. [8,24] reported that the absorption edge of N-doped TiO_2 could be red-shifted to 404 nm and that the N-doped TiO_2 had good photocatalytic activity under visible light irradiation. However, due to strongly localized N 2p states at the top of valence band, the photocatalytic efficiency of N-doped TiO_2 decreases because isolated empty states tend to trap photogenerated electrons, thereby reducing the photogenerated current [25]. Recently, co-doped TiO_2 with two different elements, especially nonmetal and metal elements co-doping has become a rapidly growing field of interest for computational studies. Gai et al. [26] proposed using passivated co-doping of nonmetal and metal elements to extend the TiO_2 absorption edge to the visible light range; because the defect bands are passivated, they will not be active as carrier recombination centers [27]. Because TiO_2 doped with Fe^{3+} forms electron or hole traps to reduce the recombination probability of photon generated electron–hole pairs [28].

Sonochemistry has proven to be an excellent method in the preparation of amorphous and crystalline nanosized materials [29,30]. The collapse of bubbles generates localized hot spots with transient temperatures of above 5000 K, pressure of about 20 MPa, and heating and cooling rates greater than $10^9\ K\ s^{-1}$ [31]. These extreme conditions can obviously accelerate the hydrolysis or condensation reaction.

* Corresponding author. Tel.: +82 41 530 2364; fax: +82 41 530 2840.
E-mail address: swlee@sunmoon.ac.kr (S.-W. Lee).

0920-5861/$ – see front matter © 2012 Elsevier B.V. All rights reserved.
http://dx.doi.org/10.1016/j.cattod.2012.09.014

In the present study, the sonochemical method was used to prepare Fe–N–TiO_2 photocatalysts with the assistance of high power ultrasound. The photocatalytic activity of the Fe–N–TiO_2 was tested by degradation of indigo carmine dye (ICD) in aqueous model solution under solar light irradiation.

2. Experimental

2.1. Preparation of the photocatalyst

Nitrogen doped anatase TiO_2 crystalline phase was prepared by drop-wise addition method, similar to that used for only N-doped TiO_2 reported in a previous paper [32]. An aqueous solution 1 M titanium sulfate (Kanto Chemical 97%) was hydrolyzed by the addition of ammonium hydroxide (J.T. Baker 28%) until the pH of the mixture reached 7. The obtained hydrolysis product was washed with distilled water several times until no SO_4^{2-} was detected by adding 0.2 M $Ba(NO_3)_2$ solution to the washing solution. The washed products were further dried in a freeze dryer under continuous pumping overnight at 193 K for 24 h. After drying, the product was calcined at 673 K for 2 h in airflow to obtain yellow colored vis-active N–TiO_2 powder of anatase structure.

Fe–N–TiO_2 photocatalyst was synthesized by sonochemical method of $TiO_{2-x}N_y$ with iron (III) chloride hexahydrate (Sigma–Aldrich, 97%) and citric acid (Tokyo Chemical Industry Co., Ltd) in a mixture of degassed ethanol, and exposed to ultrasonic irradiation (20 kHz, 600 W) for 2 h. First, iron (III) chloride hexahydrate and citric acid were added to degassed ethanol and placed in ultrasonic irradiation for 10 min to assure its complete disaggregation. Then, $TiO_{2-x}N_y$ were added to the mixture and placed in ultrasonic irradiation. The obtained precipitate was washed with ethanol and distilled water. The washed products were further dried in a freeze dryer under continuous pumping overnight at 193 K for 24 h. After drying, the product was calcined at 673 K for 2 h in air. The samples were identified as N–TiO_2 for the N doped and Fe–N–TiO_2 for the N and Fe co-doped sample.

2.2. Characterization

The crystalline structure of the synthesized powders were determined by X-ray diffraction (XRD, RIGAKU D/MAX2200HR diffractometer) analysis using a Cu Kα radiation (λ = 1.5406 Å). The diffuse reflectance spectroscopy (DRS, JASCO V-570) spectra were obtained on a UV–vis spectrophotometer equipped with a reflectance sphere. The Brunauer–Emmett–Teller (BET, ASAP 2020) surface areas (S_{BET}) of the samples were analyzed by nitrogen physisorption on a nitrogen adsorption apparatus at 77 K (Micromeritics Instruments). Fourier transformed-infrared (FT-IR, JASCO FT/IR-460 Plus) spectra were measured on FT-IR spectrometer on the transmission mode using the KBr pellet technique. The determination chemical composition of the synthesized powder was performed by X-ray photoelectron spectroscopy (XPS, Ulvac-PHI 5000 VersaProbe). The spectrometer was operated in a constant pass energy mode with a monochromatized AlKα (1486.6 eV) source. The X-ray source was operated at 25 W, 15 kV The binding energies (BE) were referenced to the C1s peak, whose BE was fixed at 284.6 eV The high resolution transmission electron microscopy (HR-TEM, FEI Tecnai F30) images were obtained with a Super-win equipped with a LaB6 emission gun operating at 300 kV The point-to-point resolution is 0.24 nm and the information limit is 0.14 nm The HR-TEM digital images were obtained with a CCD camera and the Digital Micrograph Software from GATAN. The elemental composition of the samples was determined by energy dispersive X-ray spectroscopy (EDS) with an EDAX spectrometer fitted to the TEM.

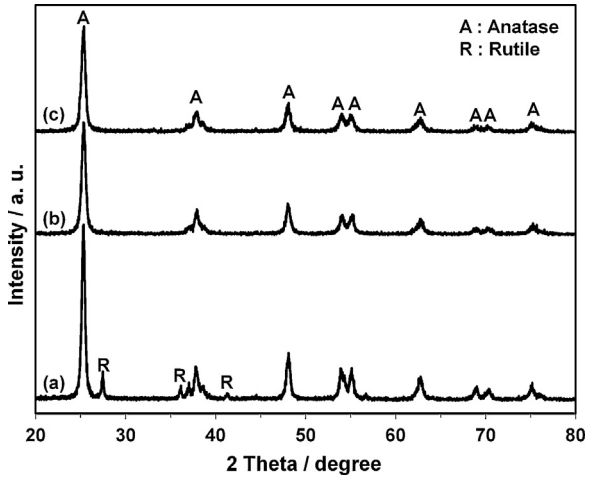

Fig. 1. XRD patterns of photocatalysts: (a) TiO_2–P25, (b) N–TiO_2 and (c) Fe–N–TiO_2.

The powdered samples were ultrasonically dispersed in isopropyl alcohol and supported on holey carbon coated copper grids.

2.3. Evaluation of photocatalytic activity

Photocatalytic degradation experiments were carried out in a petri dish reactor irradiated under solar light and visible light. Solar light irradiation was carried out using solar simulator (Portable Solar Simulator PEC-L01, Pecell) (Am 1.5G). A 40 W halogen lamp was used as the visible light source. The short wavelength components (λ < 420 nm) of the light were cut off using a glass filter. For each experiment, 50 mL of an aqueous solution of indigo carmine dye (ICD) (20 ppm) were placed inside the petri dish coated with 100 mg photocatalytic powder into a thin layer. For this, photocatalyst powder was placed in petri dish and then dispersed in absolute ethanol and ultrasonicated for 10 min The solution with dispersed photocatalyst was then dried for 24 h in an oven at 343 K. Samples for analysis were taken at different times to analyse the advance of the reaction by UV–vis analysis (MECASYS Optizen 2120UV Spectrophotometer). After that, samples were analyzed by UV–vis spectroscopy in order to follow the photocatalytic reaction. The concentration of indigo carmine dye (ICD) in the solution was determined as a function of irradiation time from the main absorbance band at a wavelength of 610 nm

3. Results and discussion

Fig. 1 shows the XRD patterns of the as-synthesized powders. The X-ray diffraction peaks of Fe–N–TiO_2 and N–TiO_2 photocatalysts are well assigned to the anatase TiO_2 crystalline phase (JCPDS 84-1286), no peaks for the rutile and brookite phases were detected. For comparative purpose the XRD pattern of TiO_2–P25 is included in Fig. 1, which clearly shows the presence of typical anatase and rutile (JCPDS 21-1276) TiO_2 crystalline phases. Further observation shows that with Fe and N doped TiO_2, XRD peak intensities of anatase steadily become weaker and wider, indicating the formation of smaller TiO_2 crystallites. Using the full width at half maximum of peak of anatase ($2\theta = 25.4^\circ$) assigned to the (1 0 1) plane diffraction, the anatase crystallite sizes of the samples were calculated by using the Scherrer equation (Table 1). Smaller crystallite size were obtained for co-doped sample, it means that the incorporation of Fe and N ions restricts the growth of TiO_2 crystallite and preventing the transformation of anatase to rutile crystalline phase. However, the diffraction patterns of Fe or Fe_xO_y, phases were not detected by XRD [33,35]. One probable reason is either the concentration of Fe, N co-doping was lower than the